Nanocatalysis

International Edition: DOI: 10.1002/anie.201912241
German Edition: DOI: 10.1002/ange.201912241

Electrochemically Tunable Proton-Coupled Electron Transfer in Pd-Catalyzed Benzaldehyde Hydrogenation

Katherine Koh[+], Udishnu Sanyal[+], Mal-Soon Lee, Guanhua Cheng, Miao Song, Vassiliki-Alexandra Glezakou, Yue Liu, Dongsheng Li, Roger Rousseau, Oliver Y. Gutiérrez, Abhijeet Karkamkar,* Miroslaw Derewinski, and Johannes A. Lercher**

Abstract: *Acid functionalization of a carbon support allows to enhance the electrocatalytic activity of Pd to hydrogenate benzaldehyde to benzyl alcohol proportional to the concentration of Brønsted-acid sites. In contrast, the hydrogenation rate is not affected when H_2 is used as a reduction equivalent. The different responses to the catalyst properties are shown to be caused by differences in the hydrogenation mechanism between the electrochemical and the H_2-induced hydrogenation pathways. The enhancement of electrocatalytic reduction is realized by the participation of support-generated hydronium ions in the proximity of the metal particles.*

Carbon is a widely used catalyst support that combines chemical and structural diversity with electrical conductivity.[1–3] Contrary to the common notion of its chemical inertness, modified carbon materials impact catalytic reactions through electronic and acid–base-induced interactions with supported metal nanoparticles.[4–6]

[*] Dr. K. Koh,[+] Dr. U. Sanyal,[+] Dr. M.-S. Lee, Dr. V.-A. Glezakou, Dr. R. Rousseau, Dr. O. Y. Gutiérrez, Dr. A. Karkamkar, Dr. M. Derewinski, Prof. J. A. Lercher
Institute for Integrated Catalysis
Pacific Northwest National Laboratory
Richland, Washington 99352 (USA)
E-mail: oliver.gutierrez@pnnl.gov
abhi.karkamkar@pnnl.gov

Dr. G. Cheng, Dr. Y. Liu, Prof. J. A. Lercher
Department of Chemistry and Catalysis Research Center
TU München
Lichtenbergstrasse 4, 85747 Garching (Germany)
E-mail: johannes.lercher@ch.tum.de

Dr. M. Song, Dr. D. Li
Physical and Computational Sciences Directorate
Pacific Northwest National Laboratory
Richland, Washington 99352 (USA)

Dr. M. Derewinski
Jerzy Haber Institute of Catalysis and Surface Chemistry
Polish Academy of Sciences
30-239 Cracow (Poland)

[+] These authors contributed equally to this work.

Supporting information and the ORCID identification number(s) for the author(s) of this article can be found under: https://doi.org/10.1002/anie.201912241.

To influence these interactions, several methods have been reported for altering the surface properties and morphology of carbon.[7–8] Functionalization approaches include oxidation using acids, plasma treatment with O_2 and ozone, as well as thermal treatment with air to introduce oxygen-containing functional groups that increase the hydrophilicity and surface acidity.[9–13] Nitrogen-containing functional groups generated by treating carbon with NH_3 introduce basic sites.[2,14] The structure of carbon supports is tailored by carbonization of organic precursors and templating methods. For the latter, the carbon precursors are incorporated into porous templates and carbonized under inert gas, generating porous carbons.[2,15,16]

Here, we applied three approaches to modify the chemical and physical properties of carbon supports, that is, acid treatment, carbonization of N- and O-precursors, and O_2 plasma treatment. Pd nanoparticles (NPs) supported on these modified carbons were studied in the selective electrocatalytic hydrogenation (ECH) of benzaldehyde to benzyl alcohol.[17–20] The high selectivity of Pd in the ECH of benzaldehyde[21–22] simplifies the interpretation of the impact of the carbon support on the activity and selectivity of Pd.[21]

Carbon felt (CF) was used to support Pd because of its robustness[23] and large pores, which allow the facile transport of reactants. Details of the carbon modifications and catalyst synthesis are compiled in the Supporting Information (Scheme S1). Carbonization of polyaniline (PANI) or sucrose on the carbon felt introduced N- or O-containing functionalities, respectively (denoted as PANI CF and Sucrose CF). The specific surface area of the carbonized layer on the felt was varied by using colloidal SiO_2 (Ludox® HS-40)[16] as a sacrificial template during the carbonization process. While in the absence of SiO_2, the specific surface area of the felts increased from 1 to 32 $m^2 g^{-1}$ by carbonization of the organic precursors (entries 1, 2, and 4 in Table 1), SiO_2 templating introduced additional microporosity (for N_2-sorption isotherms, see Figure S1 and Table S1), increasing the specific surface area of the felts to approximately 110 $m^2 g^{-1}$ (entry 3 and 5 in Table 1). Materials with carboxylic, phenolic, and carbonyl groups (Table 1, Figures 1 and S2) were prepared by oxidation with nitric acid or by O_2 plasma treatment (Section S1 in the Supporting Information).

Using C 1s X-ray photoelectron spectroscopy (XPS) and Boehm titration,[24–25] we quantified the concentration of oxygen-containing functional groups and the surface acidity. The total surface acidity (including carboxylic, phenolic, and lactonic groups) as measured by Boehm titration increased

Table 1: Physical and chemical properties of parent and modified carbon felts.

Entry		S_{BET}[a] [$m^2 g^{-1}$]	Total acidity[b] [$\mu mol\, g^{-1}$]	Relative area in C 1s XPS [%]		
				R–COOH	R–OH	C=O
1	Parent CF	1	40	0.7	10.5	3.8
2	PANI CF (low)	28	140[e]			
3	PANI CF[c]	110	170[e]	6.3[f]	17.9[f]	9.4[f]
4	Sucrose CF (low)	36	180[e]			
5	Sucrose CF[c]	111	200[e]	3.2	12.5	6.0
6	HNO_3 CF[d]	35	200	2.9	14.0	5.9
7	O_2-plasma CF	3	280	5.8	12.7	17.3

[a] Obtained from N_2 adsorption/desorption isotherms; [b] Total acidity (carboxylic, phenolic, lactonic) from Boehm titration; [c] Carbonization with hard template (®Ludox HS-40); [d] Prepared by treatment in HNO_3 for 12 h; [e] CF prepared by carbonization method (from O_2 plasma CF with PANI or Sucrose solution); [f] The corresponding signals overlap with N-groups, for example, C–NH/C–OH, C=N/C=O.

from 40 $\mu mol\, g^{-1}$ (Parent CF) to 140–280 $\mu mol\, g^{-1}$ upon modification (Table 1).

For the felt treated by carbonization with PANI, the C 1s XPS signals of oxygen-containing functional groups overlap with the signals of the C–N bonds (Table 1).[26] N 1s XPS showed the presence of pyridinic, pyrrolic, quaternary, and pyridinic N^+-O^- groups in proportions of 45.3, 15.1, 33.1, and 6.4%, respectively (Figure S3).

Pd NPs were deposited on the CFs following the impregnation and thermal treatments described in the Supporting Information. The concentration of acid sites decreased upon Pd deposition (Table S2), which is attributed to a partial exchange or removal of functional groups during the reductive treatments. These changes did not affect the relative contributions of different functional groups to the total acidity (Figures S4 and S5). The average particle sizes and the fraction of accessible Pd atoms were determined by transmission electron microscopy (TEM) and chemical titration in the liquid phase (Table S3 as well as Figures 1 e,f, S6, and S7). TEM showed similar particle-size distributions with average particle sizes from 4.7 to 6.3 nm. These values agree with the fraction of accessible metal sites determined by titration with 1-butanethiol (Figure S7).[27] Since all Pd particle sizes have an average diameter of 5.2 nm and a similar concentration of Pd, particle-size effects are eliminated as a cause for the different catalytic properties.

All Pd catalysts enabled the hydrogenation of benzaldehyde to benzyl alcohol by electrocatalysis (Figure S8) and with H_2 at room temperature. A re-use of catalysts did not induce variations in the catalyst activity (Figure S9).

Pd supported on carbon with N-containing functional groups had a lower activity than Pd supported on carbons with only O-containing functional groups (Figures 2 a and S10). Among the latter, the activity increased in the sequence Pd/Sucrose CF < Pd/HNO_3 CF < Pd/O_2-plasma CF (Figure 2 a). In contrast, the felts containing nitrogen had higher HER rates than the felts with oxygen functionalities. For instance, on the Pd/PANI-modified CFs, the HER turnover frequencies (TOFs) were 386 and 233 h^{-1} (Pd/PANI CF with low and high surface area, respectively) while on the oxygen-functionalized catalysts, the HER rates were < 105 h^{-1} in all cases (Figure 2 a). Hence, the Faradaic efficiency (FE, that is, the number of electrons used for hydrogenation in relation to the total current) varied with the carbon functionality. The FE was 40–50% for the catalysts containing nitrogen and 80–95% for catalysts with only oxygen functionalities (Figure S11 a). The current densities (that is, currents normalized

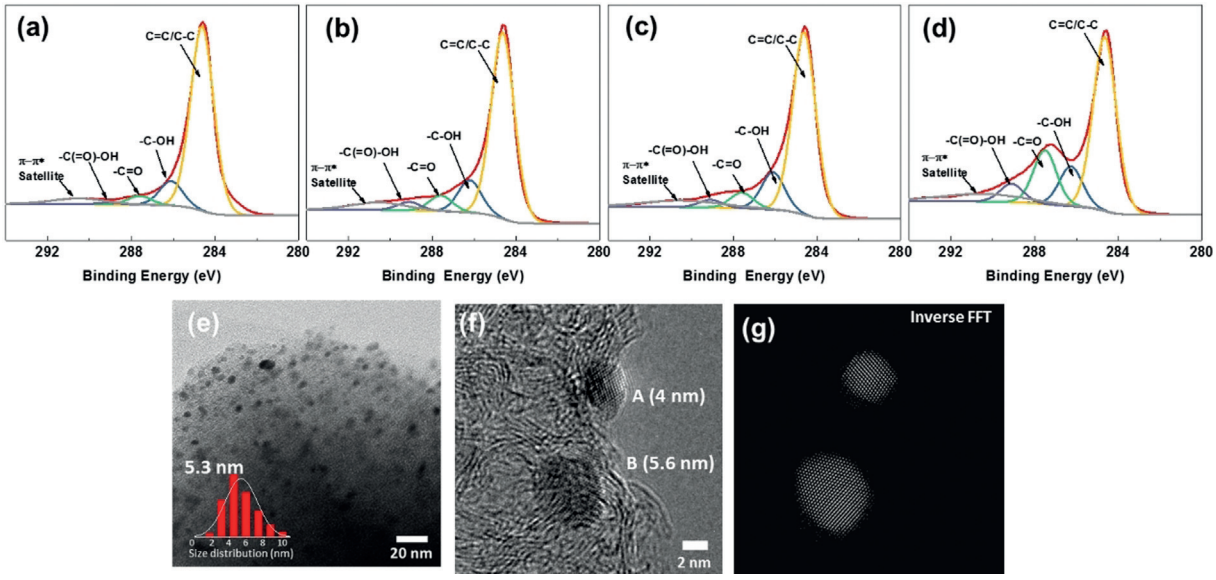

Figure 1. Characterization of catalysts: C 1s XPS of a) Parent CF, b) Sucrose CF (surface area: 110 $m^2 g^{-1}$), c) HNO_3 CF, and d) O_2-plasma CF. e) Transmission electron microscopy (TEM) image of Pd/O_2-plasma CF, f) high-resolution TEM, and g) inverse FFT of the Pd particle marked A in panel (f).

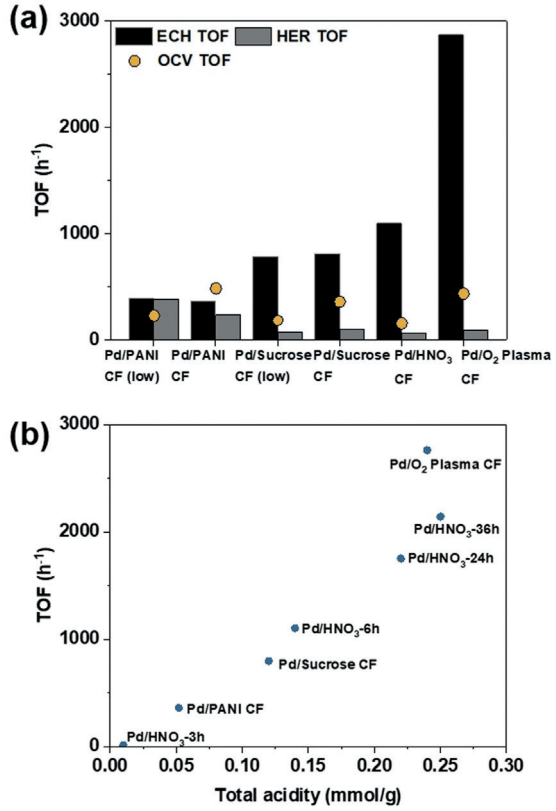

Figure 2. a) Turnover frequency (TOF) of the electrocatalytic hydrogenation (ECH), open-circuit voltage (OCV) reactions, and H_2 evolution (HER) observed during the ECH of benzaldehyde on Pd supported on functionalized felts. b) TOFs of the ECH of benzaldehyde vs. the concentration of acid sites in the Pd catalysts. Electrochemical tests were performed with solutions containing 20 mM benzaldehyde in an acetate buffer (pH 5.2) at −0.1 V vs. RHE. OCV experiments were performed with 1 bar H_2 instead of an external potential.

to the area of exposed metal), varied from $-0.05\ mA\,cm^2$ to $-0.24\ mA\,cm^2$ and were higher for O-functionalized than for N-containing carbon supports (Figure S11b).

The rates were independent of the specific surface area (Figure S10) and the porosity of the carbon support, in line with the absence of transport limitations, which was discussed in a previous work.[28] The XPS peaks of $Pd^0\ 3d_{3/2}$ and $Pd^0\ 3d_{5/2}$ were invariant among different samples. Thus, we conclude that strong electronic interactions between the support and the metal do not exist (Figure S12). The absence of systematic differences in the rate of hydrogenation with H_2 in absence of an external potential (varying randomly within the range 180–508 h^{-1}, Figure 2a) confirms that the electronic interactions between Pd and carbon are not large enough to influence the intrinsic catalytic properties of Pd.

Rates per mass of catalyst as well as rates normalized to the accessible Pd surface atoms (TOF) show direct correlations with the concentration of Brønsted-acid sites of the modified felts and Pd catalysts (Figures 2b, S13, and S14a). Remarkably, the correlation of ECH rates and concentration of acid sites in the Pd catalysts (Figures 2b and S13) indicates that both metal and acid functionalities are required for an efficient electrocatalytic hydrogenation of the carbonyl group. The method of generating Brønsted-acid sites or the presence of nitrogen in the carbon did not directly influence this dependence.

We ruled out a role of the support acidity by modifying the electronic properties of Pd because hydrogenation with H_2 showed a much weaker impact of the concentration of hydronium ions. Thus, we hypothesize that the impact on the rate of the ECH of benzaldehyde is related to the direct involvement of the acid functional groups in the proximity of the Pd particles. Such a positive impact would imply that the rate-determining step of the catalyzed reaction is related to a proton-coupled electron transfer (PCET).[21,28,29] Here, the functional group acts as a channel for the proton that is transferred from the hydronium ions in the double layer. Indeed, PCET mechanisms seem to be common in the reductive transformation of carbonyl groups.[30,31] The lack of impact on the HER in the absence of benzaldehyde allows to rule out an influence of the hydronium-ion concentration induced by the support on the rate of proton reduction (Figures S15 and S16).

Two catalysts, Pd/HNO_3CF-12h and Pd/HNO_3CF-6h, were investigated at pH 2.5, 5.2, and 10.5 (Figure S17). The ECH rates increased with decreasing pH, paralleling a recent study.[32] Importantly, the differences between both catalysts become more pronounced as the pH increases. That is, both catalysts show nearly the same rates at pH 2.5, but at higher pH, the rates of Pd/HNO_3CF-12h (which has a higher concentration of acid sites) are higher than the rates observed for Pd/HNO_3CF-6h. Thus, the local availability of hydronium ions, enhanced by the acid functional groups, generates an environment in the double layer that maintains the PCET pathway even at high pH.

The question now arises why the rates of benzaldehyde hydrogenation by H_2 (that is, under open-circuit voltage, OCV conditions) do not show a strong positive effect on the increased concentration of Brønsted-acid sites. Two models can be conceived. In the first, it is assumed that the mechanism between electrochemical and open OCV hydrogenation are identical but that the full saturation of Pd with organic compounds (the reaction order in benzaldehyde was zero) limits the reductive adsorption of H_2, thus limiting the availability of H^+–e^- pairs.[21,29,30] During electrochemical hydrogenation, this limitation does not exist, because electrons are provided by the current and the proton is readily replenished from hydronium ions of the aqueous phase. To test this hypothesis, we probed the accessibility of H_2 on Pd in a separate experiment using H_2/D_2 exchange in the aqueous phase in the presence and absence of benzaldehyde (Figure S18; for details on the method, see Section S2 in the Supporting Information). The rate of hydrogen adsorption (derived from the kinetics of the H/D exchange as detailed in the Supporting Information) during the hydrogenation of benzaldehyde dropped only by 30%. Thus, adsorbed benzaldehyde fills all its own adsorption sites but leaves enough space for dissociatively adsorbed H_2.

This leads to the second possibility, which is that in the absence of an external potential, the hydrogenation of benzaldehyde occurs via a Langmuir–Hinshelwood-type mechanism, albeit at a lower rate than achievable through

the PCET route at high Brønsted-acid-site concentrations in electrocatalysis.

Pd NPs supported on functionalized graphene were studied by ab-initio molecular-dynamics (AIMD) simulations (Figures 3 and S19). We first examined the electronic properties of the Pd NPs by computing their work functions Φ, which were determined as 4.07 and 4.12 eV for hydroxyl- and carboxylic-functionalized carbon support, respectively. The small difference in the work function ($\Delta\Phi =$ 0.05 eV) indicates that the electronic states and hence the redox properties are independent of carbon functionalization, in perfect agreement with the XPS results. We then considered the role of acid–base properties of the supports and their potential impact upon catalysis. As shown in Figure 3, the proton in the hydroxyl group requires 168 and 133 kJ mol^{-1} to be transferred to water and adsorbed benzaldehyde, respectively. This indicates that this hydroxyl proton is weakly acidic and therefore does not to play an appreciable role in the catalytic reaction. In contrast, the proton transfer from a carboxyl group to water requires only 6 kJ mol^{-1} for water and the same energy for benzaldehyde. Proton transfer between the carboxylic acid group and benzaldehyde is equilibrated with an equilibrium constant $K_{eq} = \exp(-\Delta E/k_B T) \approx 1.5$. This confirms that support functionalization with acid groups may have a strong impact on the acid–base properties of the surface and subsequently enhance catalysis.

The calculations indicate that the functional groups in the carbon support and/or the hydrated hydronium ions they generate are able to participate in the electrochemical hydrogenation. For the support-induced Brønsted-acid functionality, this must occur at the interface between Pd and the support, as shown in the hydrogenation cycle (Scheme 1). The

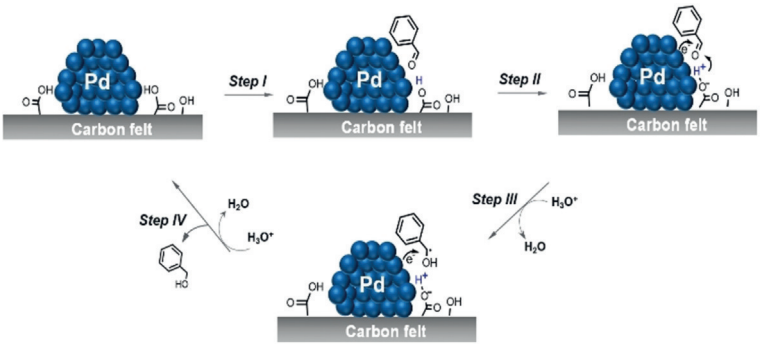

Scheme 1. Hydrogenation cycle of benzaldehyde on an acid-functionalized support with the hydrogenation steps depicted as proton-coupled electron additions: adsorption of benzaldehyde (*Step I*); sequential hydrogenation with regeneration of the Brønsted-acid site (*Step II and III*); desorption of benzyl alcohol with regeneration of the Brønsted-acid site (*Step IV*).

acid sites in the proximity of the Pd particles protonate adsorbed benzaldehyde simultaneously with the addition of electrons from the metal to complete a hydrogenation step.

In conclusion, the functionalization of carbon supports with acid groups enhances the rate of electrochemical hydrogenation of carbonyl groups in the aqueous phase. This effect becomes stronger as the concentration of hydronium ions in solution decreases. Thus, Brønsted-acid sites in the proximity of the metal particles open a robust new catalytic route for the ECH of benzaldehyde via a proton-coupled electron transfer that is inaccessible if the hydrogenation is performed with H_2 only. This insight opens new pathways for selective organic transformations and the low-temperature reductive manipulation of functional groups.

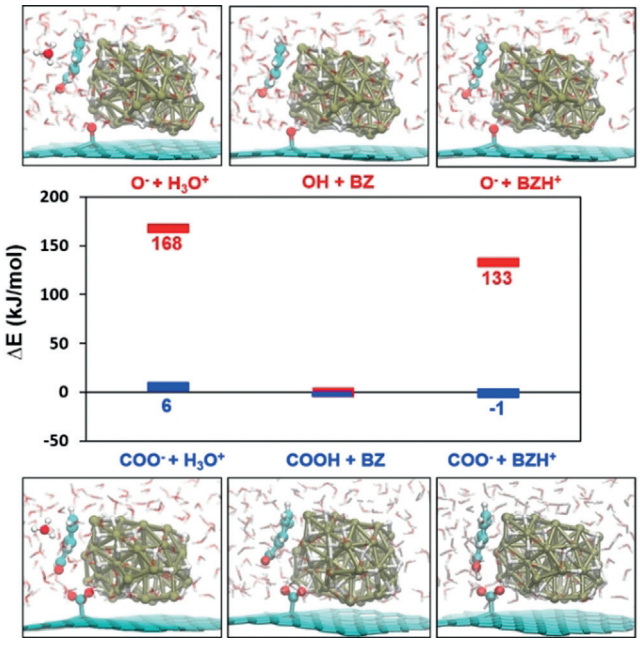

Figure 3. Relative energies (middle panel) and their optimized structures of Pd NPs on hydroxyl- (upper panel) and carboxyl-functionalized (lower panel) graphene obtained by AIMD simulations. BZ: benzaldehyde, BZH^+: protonated benzaldehyde. Color code: red, oxygen; cyan, carbon; olive, Pd.

Acknowledgements

The research described in this paper is part of the Chemical Transformation Initiative at Pacific Northwest National Laboratory (PNNL), conducted under the Laboratory Directed Research and Development Program at PNNL, a multi-program national laboratory operated by Battelle for the U.S. Department of Energy. Computational resources were provided by PNNL Research Computing. O.Y.G. and M.D. were supported by the U.S. Department of Energy (DOE), Office of Science, Office of Basic Energy Sciences (BES), Division of Chemical Sciences, Geosciences and Biosciences (Transdisciplinary Approaches to Realize Novel Catalytic Pathways to Energy Carriers, FWP 47319). J.A.L. was funded by the Deutsche Forschungsgemeinschaft (DFG, German Research Foundation) under Germany's Excellence Strategy—EXC 2089/1-390776260.

Conflict of interest

The authors declare no conflict of interest.

Keywords: acidity of support · biomass conversion · carbon modification · electrocatalytic hydrogenation · nanocatalysis

How to cite: *Angew. Chem. Int. Ed.* **2020**, *59*, 1501 –1505
Angew. Chem. **2020**, *132*, 1517 –1521

[1] D. H. Su, G. Centi, *J. Energy Chem.* **2013**, *22*, 151.
[2] J. L. Figueiredo, *J. Mater. Chem. A* **2013**, *1*, 9351.
[3] E. Frackowiak, F. Beguin, *Carbon* **2001**, *39*, 937.
[4] H.-S. Oh, H. N. Nong, T. Reier, A. Bergmann, M. Gliech, J. Ferreira de Araújo, E. Willinger, R. Schlögl, D. Teschner, P. Strasser, *J. Am. Chem. Soc.* **2016**, *138*, 12552.
[5] C. Jackson, G. T. Smith, D. W. Inwood, A. S. Leach, P. S. Whalley, M. Callisti, T. Polcar, A. E. Russell, P. Levecque, D. Kramer, *Nat. Commun.* **2017**, *8*, 15802.
[6] R. G. Rao, R. Blume, T. W. Hansen, E. Fuentes, K. Dreyer, S. Moldovan, O. Ersen, D. D. Hibbitts, Y. J. Chabal, R. Schlögl, J.-P. Tessonnier, *Nat. Commun.* **2017**, *8*, 340.
[7] G. Centi, K. Barbera, S. Perathoner, N. K. Gupta, E. E. Ember, J. A. Lercher, *ChemCatChem* **2015**, *7*, 3036.
[8] N. K. Gupta, B. Peng, G. L. Haller, E. E. Ember, J. A. Lercher, *ACS Catal.* **2016**, *6*, 5843.
[9] J. J. Ternero-Hidalgo, J. M. Rosas, J. Palomo, M. J. Valero-Romero, J. Rodríuez-Mirasol, T. Cordero, *Carbon* **2016**, *101*, 409.
[10] C. Moreno-Castilla, M. V. Lopez-Ramon, F. Carrasco-Marin, *Carbon* **2000**, *38*, 1995.
[11] J. P. Boudou, J. I. Paredes, A. Cuesta, A. Martínez-Alonso, J. M. D. Tascón, *Carbon* **2003**, *41*, 41.
[12] H. Valdés, M. Sánchez-Polo, J. Rivera-Utrilla, C. A. Zaror, *Langmuir* **2002**, *18*, 2111.
[13] J. L. Figueiredo, M. F. R. Pereira, M. M. A. Freitas, J. J. M. Órfão, *Carbon* **1999**, *37*, 1379.
[14] B. Stöhr, H. P. Boehm, R. Schlögl, *Carbon* **1991**, *29*, 707.
[15] C. O. Ania, V. Khomenko, E. Raymundo-Piñero, J. B. Parra, F. Béguin, *Adv. Funct. Mater.* **2007**, *17*, 1828.
[16] K. Koh, M. Jeon, D. M. Chevrier, P. Zhang, C. W. Yoon, T. Asefa, *Appl. Catal. B* **2017**, *203*, 820.
[17] S. Jung, E. J. Biddinger, *ACS Sustainable Chem. Eng.* **2016**, *4*, 6500.
[18] Z. R. Ismagilov, E. V. Matus, I. Z. Ismagilov, O. B. Sukhova, S. A. Yashnik, V. A. Ushakov, M. A. Kerzhentsev, *Catal. Today* **2019**, *323*, 166.
[19] X. H. Chadderdon, D. J. Chadderdon, J. E. Matthiesen, Y. Qiu, J. M. Carraher, J.-P. Tessonnier, W. Li, *J. Am. Chem. Soc.* **2017**, *139*, 14120.
[20] U. Sanyal, J. Lopez-Ruiz, A. B. Padmaperuma, J. Holladay, O. Y. Gutiérrez, *Org. Process Res. Dev.* **2018**, *22*, 1590.
[21] Y. Song, U. Sanyal, D. Pangotra, J. D. Holladay, D. M. Camaioni, O. Y. Gutiérrez, J. A. Lercher, *J. Catal.* **2018**, *359*, 68.
[22] J. D. Egbert, J. A. Lopez-Ruiz, S. Prodinger, J. D. Holladay, D. M. Mans, C. E. Wade, R. S. Weber, *J. Catal.* **2018**, *365*, 405.
[23] J. González-García, P. Bonete, E. Expósito, V. Montiel, A. Aldaz, R. Torregrosa-Maciá, *J. Mater. Chem.* **1999**, *9*, 419.
[24] H. P. Boehm, *Carbon* **1994**, *32*, 759.
[25] S. L. Goertzen, K. D. Thériault, A. M. Oickle, A. C. Tarasuk, H. A. Andreas, *Carbon* **2010**, *48*, 1252.
[26] R. Silva, D. Voiry, M. Chhowalla, T. Asefa, *J. Am. Chem. Soc.* **2013**, *135*, 7823.
[27] U. Sanyal, Y. Song, N. Singh, J. L. Fulton, J. Herranz, A. Jentys, O. Y. Gutiérrez, J. A. Lercher, *ChemCatChem* **2019**, *11*, 575.
[28] J. A. Lopez-Ruiz, U. Sanyal, J. Egbert, O. Y. Gutiérrez, J. Holladay, *ACS Sustainable Chem. Eng.* **2018**, *6*, 16073.
[29] D. C. Cantu, A. B. Padmaperuma, M.-T. Nguyen, S. A. Akhade, Y. Yoon, Y.-G. Wang, M.-S. Lee, V.-A. Glezakou, R. Rousseau, M. A. Lilga, *ACS Catal.* **2018**, *8*, 7645.
[30] C. J. Bondue, F. Calle-Vallejo, M. C. Figueiredo, M. T. M. Koper, *Nat. Catal.* **2019**, *2*, 243.
[31] C. J. Bondue, M. T. M. Koper, *J. Catal.* **2019**, *369*, 302.
[32] N. Singh, M.-S. Lee, S. A. Akhade, G. Cheng, D. M. Camaioni, O. Y. Gutiérrez, V.-A. Glezakou, R. Rousseau, J. A. Lercher, C. T. Campbell, *ACS Catal.* **2019**, *9*, 1128.

Manuscript received: September 25, 2019
Accepted manuscript online: October 21, 2019
Version of record online: December 12, 2019

